

Experimental Research on Impinging Slot Jet on a Concave Surface – Effects of Impinging Height and Reynolds Number

Nghiên cứu thực nghiệm tia khí 2D làm mát thành cong lõm
- Ảnh hưởng của độ cao làm mát và số Reynolds

Hoang Thi Kim Dung

Hanoi University of Science and Technology, No. 1, Dai Co Viet, Hai Ba Trung, Hanoi, Viet Nam

Received: March 06, 2017; accepted: June 5, 2017

Abstract

Experimental research of single slot impinging jet upon a concave surface were conducted by classical Particle Image Velocimetry (PIV) and infrared thermography. Main parameters of this research were nozzle exit Reynolds number ($Re_b = 1400-6400$), dimensionless impinging height ($H/b = 3-7$), relative curvature of wall ($D_o/b = 5$) and little dissymmetric outlet flow ($e/b = 0.8$). Results indicated that impinging jet oscillated at three semi-stable different point at high impinging height while it stabilized at a position at small impinging height. Therefore, oscillation of impinging jet generated a uniform heat transfer at high impinging height while stabilized impinging jet caused an asymmetric heat transfer at low impinging height.

Keywords: Impinging jet, concave surface, PIV, infrared thermography.

Tóm tắt

Nghiên cứu thực nghiệm tia khí 2D phun trực tiếp lên thành cong lõm được tiến hành bằng cách đo vận tốc hình ảnh hạt phân tử cổ điển (PIV) và đo nhiệt độ bằng hồng ngoại. Các thông số chính là số Reynolds đầu ra của tia khí ($Re_b = 1400-6400$), chiều cao phun không thứ nguyên ($H/b = 3-7$), độ cong tương đối của thành cong ($D_o/b = 5$) và bất đối xứng nhẹ tại dòng ra ($e/b = 0,8$). Kết quả cho thấy tia khí vẫy tại ba điểm bán-ổn định khác nhau ở chiều cao phun lớn trong khi tia khí ổn định tại một vị trí khi độ cao phun nhỏ. Vì thế, tia khí vẫy tạo ra một phân bố nhiệt đồng nhất ở chiều cao phun lớn trong khi tia khí ổn định lại tạo ra sự bất đối xứng của phân bố nhiệt ở chiều cao phun thấp.

Từ khóa: Tia phun trực tiếp, bề mặt lõm, PIV, đo nhiệt độ bằng hồng ngoại

1. Introduction

Air jets provide an effective mean for cooling surfaces of various geometries. Jet dynamics and flow structures must be studied to understand and optimize obtained heat transfer with impinging jet. Most of studies of impinging jet have focused on flat surfaces because of their strong potential concerning thermal transfers [1]. Recently, the interest moves on impingement with presence of curved (convex/concave) surfaces. Indeed, the exact role of curvature on transfer of mass and/or heat remains still badly known. To approach this problematic, we have undertaken aero-thermal research on flow which is generated by one or more impinging jets on a concave surface.

Using particle image velocimetry (PIV), Gilard & Brizzi [2] remarked a presence of three semi-stable flow regimes in vicinity of concave wall at large dimensionless impinging height. These regimes

generated a uniform heat transfer on a flat plate by using slot impinging jet (numeric study [3]). At small dimensionless impinging height, jet stabilized at center of concave wall which was called stagnation point. According to Yang & al. [4], thermal transfer was maximal at stagnation point and corresponded to location where maximum of turbulence intensity was.

Moreover, Hoang & al. (aerodynamic research [5]; thermal research [6]; comparison between aerodynamic and thermal research [7]) noticed that oscillation of impinging slot jet observed in [2] was controllable by varying outlet condition. A flow recirculation, which caused an increase of fluid temperature close to the wall, was observed. This recirculation could be appreciably changed with outlet condition. Heat transfer coefficient was estimated from nozzle exit temperature, so the raise in jet temperature would cause a drop of heat transfer. Hoang et al. [5-7] also noted that impinging height had an important role on behavior of jet. At small impinging height, jet velocity was still high; it mixed significantly with entrained air, and induced

* Corresponding author: Tel.: (+84) 949.737.767
Email: dung.hoangthikim@hust.edu.vn

turbulence and eddy activity, all of which enhance heat transfer, hence its high value.

Interest of all authors quoted above concern the impact of single slot jet on a curved wall (concave/convex). In order to use this kind of jet to optimize the cooling of a concave surface, we proposed to study, in this paper, effect of impinging height and Reynolds number with a small dissymmetric of outlet flow. Dynamics and structure of impinging slot jet was encountered by using classical PIV. And, an infrared thermography was used to carry out thermal transfer.

2. Experiment apparatus

2.1. Experimental set-up

Impinging slot jet was supplied by a right-angled parallelepiped channel (955 mm length, 300 mm width and 10 mm height). A grid and a honeycomb were placed upstream in order to make uniform the flow.

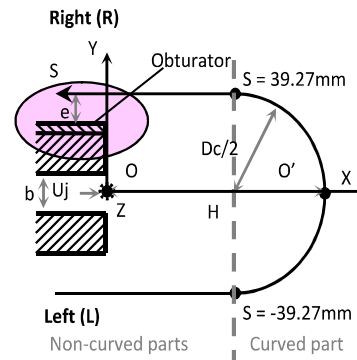
Impingement surface consisted into two parts: One was a semi-cylindrical shape (450 mm length and 50 mm diameter), simple geometry for modeling, and corresponded to curved part of impingement surface; the other was straight (450 mm length and 140 mm width), to avoid external disturbances which would contaminate jet (Fig. 1a). Impingement surface was closed laterally by transparent plates (thickness of 10 mm). All of these elements were transparent (Altuglas 3 mm thick) in order to do measurements by classical PIV velocimetry. Heating plate (epoxy/copper 0.2 mm thick, whose thermal conductivity was 0.29 ± 0.02 W/mK in thick direction) allowed thermal measurement (heat thin foil technique, infrared thermography) (Fig. 1b). Concave surface was fixed on a moving system that could vary impinging height H (H was distance between nozzle exit and center of the impingement surface).

This testing apparatus comprised of an air feed system established by a fan F 802 ($2 \text{ m}^3/\text{min}$ under 1000 mm EC, 3.9 kW, 2910 rpm) or a centrifugal fan HP APE 801C ($3 \text{ m}^3/\text{min}$, 11368 Pa, 5.3 kW, 2900 rpm) respectively to dynamic measurements and thermal measurements.

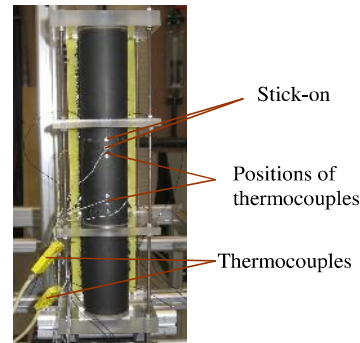
For dynamic measurements, air flow rate Q_j was controlled using manual valves and three different flowmeters Fischer & Porter connected in parallel, these flowmeters had different measurement ranges in order to optimize accuracy of aerodynamic measurements. For the part of thermal measurements, air flow rate was measured by a venturi meter. The venturi was equipped with two pressure sensors (a differential pressure (0-5 mbar) and a static pressure (800-1200 mbar)). In plus, a thermocouple

(Chromel/Alumel) was used to measure flow temperature through the venturi. This temperature was controlled by a heat exchanger placed between flowmeters and channel. Finally, all elements of this feeding system (fan, valves, flowmeters and thermal regulator) were integrated using pipe of PVC or flexible plastic of 80 mm diameter. The feeding system was connected to channel by a diffuser.

In this paper, main experimental parameters were nozzle exit Reynolds number $Re_b = 1400, 3200, 6400$ ($Re_b = U_j \cdot b / \nu$ where U_j was injected velocity, b was height of slot jet ($b = 10 \text{ mm}$) and ν was kinematic viscosity of air); dimensionless impinging height $H/b = 3, 5, 7$; and relative curvature $Dc/b = 5$. Right exit was adjusted an obturator with height of 2 mm, so open of right exit was $e/b = 0.8$ (Fig. 1a).



a. 2D view



b. Impinging surface

Fig. 1. Impinging surface

2.2. Classical PIV

Velocity was measured by using particle image velocimetry technique (LAVISION technology). An Nd-Yag doubles cavity QUANTEL laser source ($2 \cdot 120 \text{ mJ}$, 10 Hz and 532 nm) was used to illuminate flow by a relatively fine luminous plan (1.5 mm). Flow was seeded by using a generator of olive oil droplets (average diameter about $1 \mu\text{m}$).

Pictures were taken using Flowmaster CCD camera (12 bits, 1376x1040 pixels, double frames, 4-5 Hz). Recorded images were analyzed in order to obtain displacement of tracers, and then velocity. For this treatment, we used a multi-pass inter-correlation (4 passes, the last being doubled, start by 128x128 and finish by 32x32), with an overlap 50%x50%.

As a preliminary, in order to minimize influence of reflections or other artefacts, a "basic image" was subtracted from each image before estimation of vectors. This "basic image" was obtained before recording of sequence under the same experimental conditions as for measurements but in absence of particle.

Measurements were obtained for several experimental configurations. For each configuration, 5000 independent samples of measurements were recorded at 4-5 Hz and divided into 25 packages of 200 recordings. To instantaneous fields, different validation and statistical processes were implemented to obtain mean velocity and Reynolds stresses or root mean square values. However, for areas where there were less than 1000 validated vectors, no result was presented.

2.3. Infrared thermography

Infrared thermography was carried out by an infrared matrix camera and an infrared system. Data frequency remained 50 Hz, and a series of images was recorded during a lap of 10 seconds (500 images). From acquisitions of 5 different fluxes, convective heat transfer coefficient (h) was calculated according to a linear regression method within an accuracy of $\pm 12\%$ [5]. Average Nusselt number was then encountered by integrating local Nusselt numbers over cylinder surface.

Infrared thermography combined advantage of being no-intrusive and allowed a continuous measurement of considered surface. This technique was carried out by an infrared matrix CEDIP Jade MWIR camera (InSb, 3.6-5.1 μm , 320x240 pixels) and an infrared CEDIP system (Altair & Saphir). Infrared camera counted the photons, converted them into electric power (V), and then digitized the signal (DL) to finally transform these results into temperature field (K) through calibration data. Data frequency remained 50 Hz, and a series of images was recorded using Altair software during a lap of 10 seconds (500 images). Then, an average was calculated by SAPHIR software. From acquisitions of 5 different fluxes, convective heat transfer coefficient (h) was calculated according to a linear regression method [5]. The values of h were obtained with an accuracy of $\pm 12\%$.

Average Nusselt number was then obtained by integrating local Nusselt numbers over cylinder surface as:

$$\overline{Nu} = \frac{1}{S_2 - S_1} \int_{S_1}^{S_2} Nu \cdot dS \quad (1)$$

Where $S_1 = -70$ mm and $S_2 = 70$ mm.

For heat thin foil technique, impingement side (front side) of heating plate was covered by a fine layer of copper (0.35 μm thick). Three individual electric circuits were printed on this side, which heated up impingement plate by Joule effect. Width of copper track was of 1 mm and inter-track was of 0.2 mm. These dimensions ensured a uniform heat flux density on entire front surface of the impingement plate within $\pm 5\%$ of mean heat flux density over all the electric circuits [6].

Although reflective stick-on (Fig. 1b) allowed a precise location, the change of position of camera involves an uncertainty on curvilinear coordinate ($\pm 1\text{mm}$).

Ambient temperature was encountered by averaging temperature measurement of two thermocouples chromel/alumel.

3. Results and discussion

Flow field and heat transfer were found slightly dissymmetric due to existence of an obturator at right exit (see Fig. 2 to Fig. 5).

3.1. Influence of impinging height

After injection of jet, flow was in potential core region that corresponded to a high average velocity (MOY) but low turbulence intensity (RMS). However, outside potential core region, two different behaviors were observed depending on turbulence intensity (Fig. 2).

At small impinging height, impact wall was in area of potential cone, since its length was about 5b [2]. Jet maintained its speed (Fig. 2a) and impinged directly the wall at a position slightly in lower part, because of a low closure of upper output channel ($e/b = 0.8$), and then splitted into two parts. Each part of jet followed curved wall, part went up and other went down. Therefore, impinging jet was studied in steady stream of impact [2]. Two areas of high turbulence intensity (about $0.35U_j$) were also observed in Fig. 2a. One zone was in shear layers on upper and lower border of main jet. The second was found in outer portion of wall jet. These high RMS values were generated by vortices formed in jet shear zones and converted downstream by wall jet. These observations on RMS values were in good agreement

with those obtained in [2, 5-7]. In main jet, average jet velocity was high ($MOY \approx 1.12U_j$) but level of turbulent intensity was very low ($RMS \approx 0.03U_j$). These results were in good agreement with Gauntner & al. [1]. So, at impinging height lower than potential core length, jet was located in potential area, where jet velocity was constant and equaled to injection speed; and turbulence intensity was low.

At high impinging height, jet oscillated and was characterized by a slightly uniform of turbulence intensity along the wall (RMS varied from $0.5U_j$ to $0.63U_j$; Fig. 2b, 2c); and a slightly asymmetric of average velocity in stagnation region. But, at impinging height $H/b = 5$, confinement effect (plates guards, curved wall) became more important. It intervened in main jet and thus produced a perfect

uniformity of turbulence intensity in the area ($X/b = 4.4$ & $Y/b = 0.7$) to the area ($X/b = 3.0$ & $Y/b = -2.2$) (Fig. 2b).

Turbulence intensity was found twice higher in case of oscillated jet ($RMS \approx 0.7U_j$) than that of stabilized impinging jet ($RMS \approx 0.35U_j$) (Fig. 2).

Heat transfer of small impinging height ($H/b = 3$) had a maximum value at point impact, while heat transfer of high impinging height ($H/b = 7$) was slightly uniform (Fig. 3). For high impinging height, jet oscillated between three semi-stable positions [2, 5-7] that explained apparition of two maximum heat transfer in Fig. 3. Maximum value at left exit was higher than that at right exit due to the existence of an obturator at right exit.

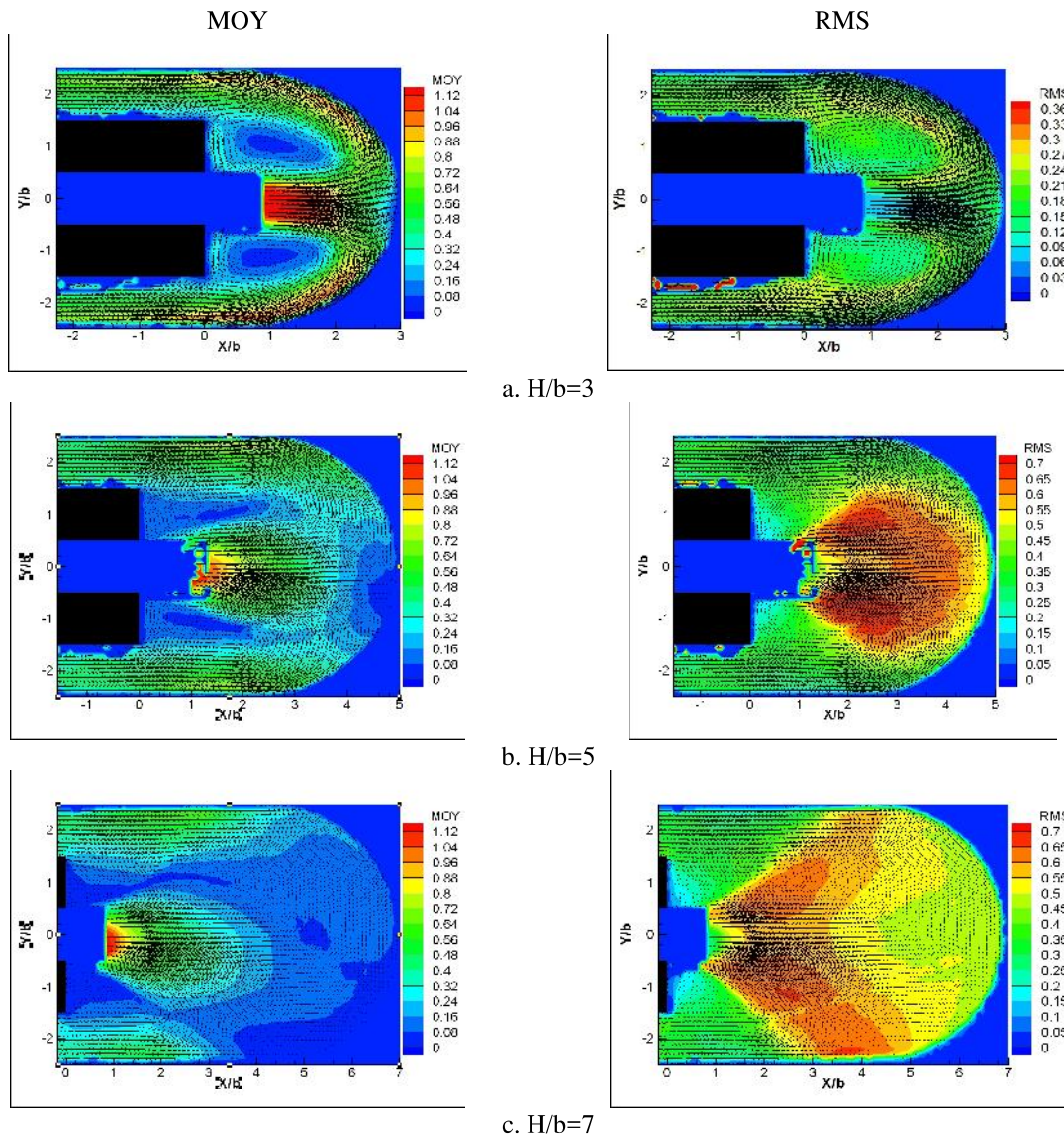


Fig. 2. Distribution of average velocity (MOY) and turbulent intensity (RMS) ($Re_b = 3200$; $D_c/b = 5$ & $e/b = 0.8$)

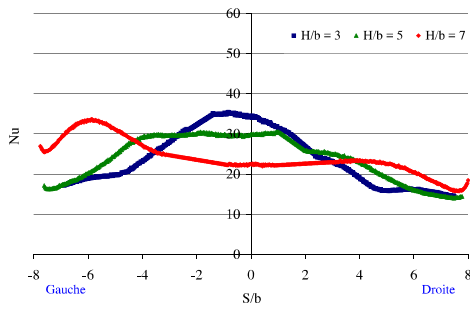


Fig. 3. Nusselt distribution ($Re_b = 3200$; $D_c/b = 5$ & $e/b = 0.8$)

Nevertheless, distribution of Nusselt number for intermediate case $H/b = 5$ remained complicate to explain. It could be an unsteady or transition effect between stabilization and oscillation of jet. In regard Fig. 2b, turbulence intensity was high and was almost

constant in region of ($X/b = 4.4$ & $Y/b = 0.7$) to ($X/b = 3.0$ & $Y/b = -2.2$). Outside this area, values of turbulence intensity decreased monotonically along impact wall. It explained why heat transfer was constant and higher in area of high turbulence intensity then decreased outside this area.

Table 1. Average heat transfer ($Re_b = 3200$)

H/b	3	5	7
\overline{Nu}	24.3	24.9	24

Average Nusselt number was about 24.5 ± 0.5 regardless of impinging height (Table 1). It seemed that effect of oscillated jet or stabilized jet had just an important role to behavior of flow field and to local heat transfer but not to average heat transfer.

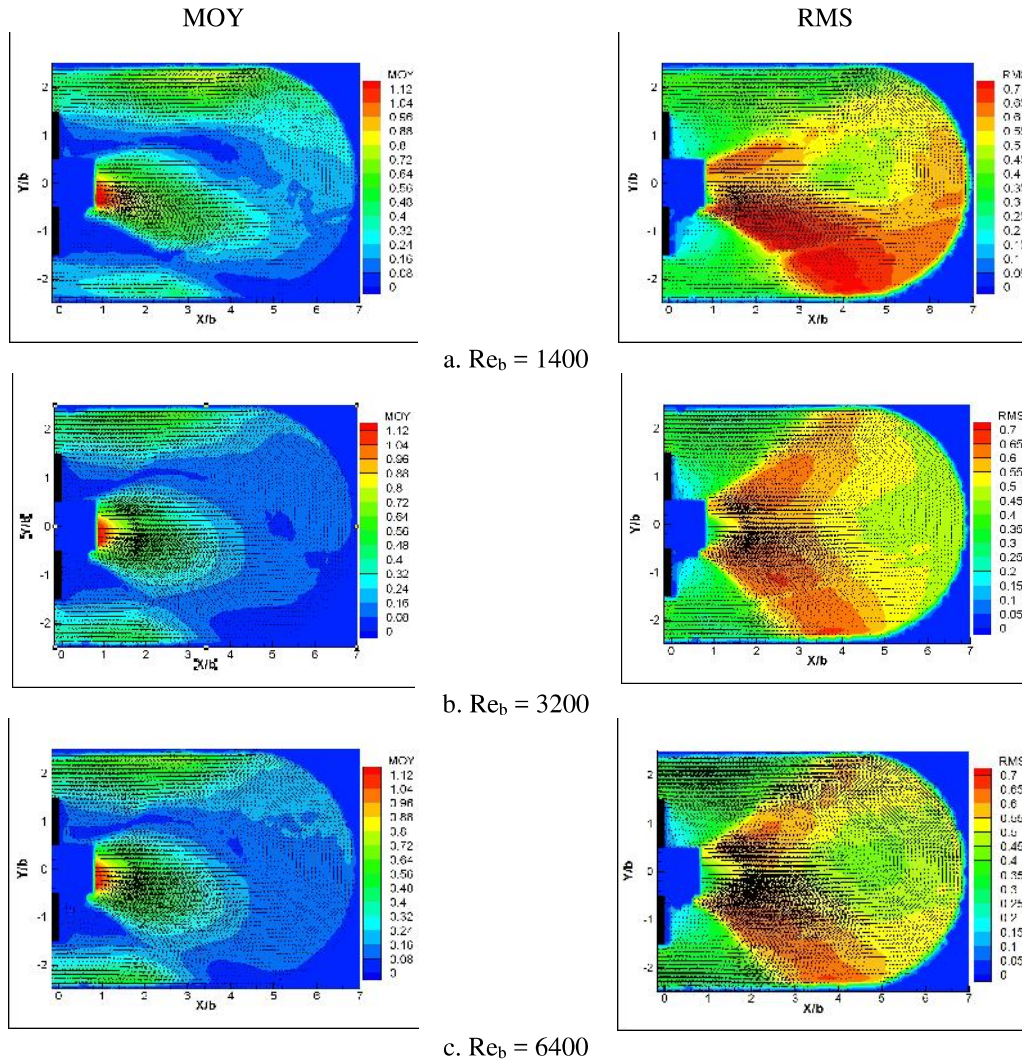


Fig. 4 Distribution of average velocity (MOY) and turbulent intensity (RMS) ($H/b = 7$; $D_c/b = 5$ & $e/b = 0.8$)

3.2. Influence of Reynolds number

Distribution of average velocity and distribution of turbulence intensity in Fig. 4 remarked that Reynolds number from 1400 to 6400 did not have a significant influence to behavior of flow field. Behavior of jet remained the same with slightly difference of average velocity ($MOY_{max} \approx 1.12U_j$) and turbulence intensity ($RMS_{max} \approx 0.7U_j$). For more details, asymmetry of turbulence intensity was notable at laminar Reynolds number ($Re_b = 1400$) (Fig. 4a). This asymmetry disappeared when jet became turbulent ($Re_b = 3200$ & 6400) (Fig. 4b, 4c).

In regard thermal field (Fig. 5), tendency of local heat transfer was the same for three studied Reynolds numbers studied. And conventionally, value of local and average heat transfer increased with the Reynolds number (Fig. 5 and Table 2).

Average value of Nusselt number could be expressed by following relationship:

$$\overline{Nu} = 0,238 Re_b^{0,58} \quad (2)$$

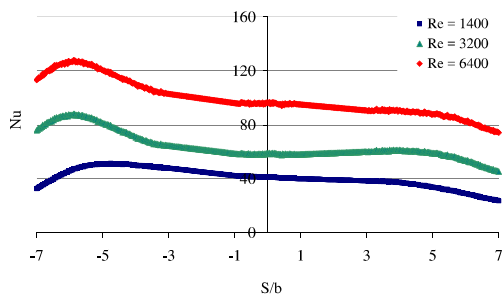


Fig. 5 Nusselt distribution ($H/b = 7$; $D_c/b = 5$ & $e/b = 0.8$)

Table 2. Average heat transfer ($H/b = 7$)

Re_b	1400	3200	6400
\overline{Nu}	15.6	24.3	37.5

4. Conclusion

The major results were summarized as follow:

- Impinging height had a strong influence on behavior of jet and local heat transfer but very weak influence to average heat transfer.

At small impinging height (stabilized jet), jet stabilized at a position and created a maximum heat

transfer at this position. The maximum value of turbulence intensity was low (about $0.35U_j$).

At high impinging jet (oscillated jet), jet impacted concave wall at three semi-stable positions and created a slightly uniform local heat transfer along impact wall. The maximum turbulence intensity of oscillated jet was twice higher than that of stabilized jet.

- Nature of jet or Reynolds number had a classic role to dynamic of jet and local and average heat transfer.

Acknowledgments

This work was carried out at Laboratory of Thermal Studies ENSMA (LET) and Aerodynamics Laboratory Studies of the University of Poitiers (LEA) under direction of Mrs. Eva Dorignac and Mr. Emmanuel Laurent Brizzi.

References

- [1] J.W. Gauntner et al., Survey of literature on flow characteristics of a single turbulent jet impinging on a flat plate, NASA Technical Note D-5652, 1970.
- [2] V. Gilard, L.E. Brizzi, Slot jet impinging on a concave curved wall, Journal of Fluids Engineering 127 (2005) 595-603.
- [3] Y.K. Suh, J.H. Park, E.C. Jeon, J.W. Kim, A numerical study on the oscillatory impinging jet, SAE 2004 Word Congress & Exhibition, 2004.
- [4] G. Yang et al., An experimental study of slot jet impingement cooling on concave surface: effects of nozzle configuration and curvature, International Journal of Heat and Mass Transfer, 42 (1999) 2199-2209.
- [5] T.K.D. Hoang, L.E. Brizzi, E. Dorignac, influence des conditions d'entrée/sortie pour un jet plan impactant une surface concave en milieu confiné, 18th Congrès Français de Mécanique, Grenoble, French, 2007.
- [6] T.K.D. Hoang, M. Fenot, L.E. Brizzi, E. Dorignac, Etude des transferts thermiques d'une paroi concave soumise à l'impact d'un jet plan en milieu confiné pour différentes conditions de sortie du jet, Société Français de Thermique, Toulouse, French, 2008.
- [7] T.K.D. Hoang, L.E. Brizzi, E. Dorignac, M. Fenot, Influence of asymmetric blockage at flow exit on flow and heat transfer for an impinging slot jet on semi-concave surface; 6th International Conference on Heat Transfer, Fluid Mechanics and Thermodynamics, Pretoria, South Africa, HT1, 2008.